

# $H_\infty$ Control of Active Suspension with Ensuring Ride Comfort

M2015SC017 Tatsuo TODA

Supervisor: Isao TAKAMI

## Abstract

This paper presents a method of the  $H_\infty$  control for an active suspension. The main purpose of this study is to ensure the ride comfort. The comfort reactions to vibration environment is defined in International Organization for Standardization (ISO) 2631-1. In this paper, the comfort reaction is introduced as the constraint. The  $L_2$  norm which is regarded as the weighted root mean square (r.m.s.) acceleration is suppressed to satisfy the constraint. On the other hand, to improve the ride comfort is also one of the purposes. The perturbation of the vertical force of the wheel which affects the lateral force is suppressed by considering the deflection of the wheel. The controller is derived by solving a finite set of Linear Matrix Inequalities (LMIs). The effectiveness of the proposed controller is evaluated by the simulation. The road surface profile based on ISO 8608 is introduced in the evaluation.

## 1 Introduction

A suspension is a component which connects a vehicle body to a wheel.

It mainly consists of the springs and dampers. It can absorb the vibration transmitted from the road surface. As the types of suspension, there are passive suspension and active suspension. The active suspension shows higher performance than passive suspension by using an actuator in addition to the springs and dampers.

The first roll of the suspension is to improve the ride comfort. According to ISO 2631-1, the ride comfort can be evaluated by the accelerations of the human body [1]. The comfort reactions to vibration environment using the weighted r.m.s. acceleration are defined in ISO 2631-1. The second roll of the suspension is to improve the driving stability. It is improved by suppressing the perturbation of the vertical force of the wheel. If there is a perturbation of the vertical force, the lateral force required for turning or stopping is also changed [2].

Recently, there are many studies which focus on both the ride comfort and the driving stability. In those studies, various control methods are proposed such as  $LQR$  control [3],  $H_\infty$  control [4], and so on. In some studies, the loop-shaping for the specific frequency range based on ISO 2631-1 is used to improve the ride comfort more effectively [4].

In this paper, The quarter vehicle model is analyzed. The main purpose of this study is to ensure the ride comfort. The comfort reaction to vibration environment defined in ISO 2631-1 is introduced as the constraint. The frequency weight based on IO 2631-1 is used. The  $L_2$  norm which is regarded as the weighted r.m.s. acceleration is suppressed to satisfy the constraint. On the other hand, to improve the driving stability is also one of the purposes. The perturbation of the vertical force of the wheel is suppressed by considering the deflection of the wheel. To satisfy those purposes, the  $H_\infty$  controller is designed. The controller is derived by solving a finite set of LMIs. The effectiveness of the proposed

controller is evaluated by simulations. The road surface profile based on ISO 8608 is introduced in the evaluation to conduct more realistic simulations [5].

## 2 Modeling

In this section, a quarter vehicle model of an active suspension shown in Fig. 1 is analyzed. The model

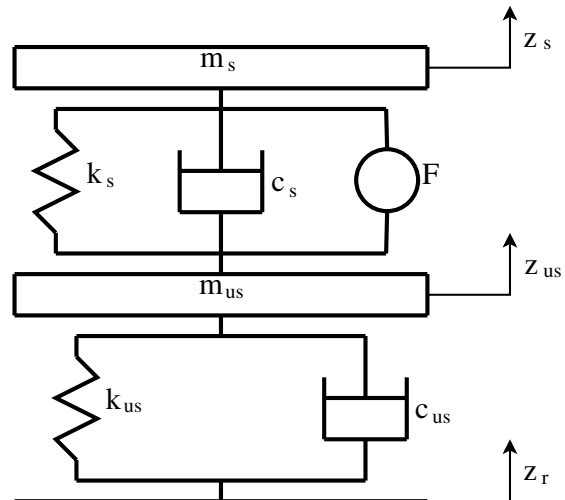


Figure 1 Quarter vehicle model

consists of three layers, which are the vehicle body, the wheel, and the road surface from the top to the bottom. They are connected by springs and dampers. There is an actuator between the vehicle body and the wheel. If there isn't control input, the active suspension works as a passive suspension.

Here  $z_s$ [m],  $z_{us}$ [m], and  $z_r$ [m] are the displacements of the vehicle body, the wheel, and the road surface from their equilibrium points, respectively.  $F$ [N] is the control input.

### 2.1 Physical Parameters

In this paper, an experimental unit which is a small scale model of a vehicle is used. The physical constants of the model are shown in Tab. 1.

Table 1 Physical constants

Description	Symbol	Value
Sprung mass	$m_s$	2.45[kg]
Unsprung mass	$m_{us}$	1[kg]
Suspension stiffness	$k_s$	970[N/m]
Wheel stiffness	$k_{us}$	2717[N/m]
Suspension damping	$c_s$	7.5[Ns/m]
Wheel damping	$c_{us}$	5[Ns/m]

### 2.2 Motion equation

The motion equations of the model are derived based on Newton's motion equation. The motion equations of

$z_s(t)$  and  $z_{us}(t)$  are derived as Eqs. (1) and (2).

$$m_s \ddot{z}_s = -k_s(z_s - z_{us}) - c_s(\dot{z}_s - \dot{z}_{us}) + F \quad (1)$$

$$m_{us} \ddot{z}_{us} = k_s(z_s - z_{us}) + c_s(\dot{z}_s - \dot{z}_{us}) - F - k_{us}(z_{us} - z_r) - c_{us}(\dot{z}_{us} - \dot{z}_r) \quad (2)$$

### 2.3 State space representation

The state space representation is derived from Eqs. (1) and (2). The state variable vector  $x(t)$ , the disturbance  $w(t)$ , the control input  $u(t)$ , and the output vectors  $y_1(t)$  and  $y_2(t)$  are defined as follows.  $y_1(t)$  represents the vertical acceleration, and  $y_2(t)$  represents the perturbation of the vertical force of the wheel and the control input. Here  $N_z$  means the perturbation of the vertical force which is calculated as  $N_z = k_{us}(z_{us} - z_r) + c_{us}(\dot{z}_{us} - \dot{z}_r)$ .

$$x(t) = [ z_{us} - z_r \quad z_s - z_{us} \quad \dot{z}_{us} \quad \dot{z}_s ]^T$$

$$w(t) = \dot{z}_r, \quad u(t) = F$$

$$y_1(t) = \ddot{z}_s, \quad y_2(t) = [ N_z \quad F ]^T$$

The state space representation  $P(s)$  is derived as Eq. (3).

$$P(s) : \begin{cases} \dot{x}(t) = Ax(t) + B_w w(t) + B_u u(t) \\ y_1(t) = C_1 x(t) + D_{u1} u(t) \\ y_2(t) = C_2 x(t) + D_{u2} u(t) \end{cases} \quad (3)$$

$$A = \begin{bmatrix} 0 & 0 & 1 & 0 \\ 0 & 0 & -1 & 1 \\ -\frac{k_{us}}{m_{us}} & \frac{k_s}{m_{us}} & -\frac{c_{us}+c_s}{m_{us}} & \frac{c_s}{m_{us}} \\ 0 & -\frac{k_s}{m_s} & \frac{c_s}{m_s} & -\frac{c_s}{m_s} \end{bmatrix}$$

$$B_w = \begin{bmatrix} -1 \\ 0 \\ \frac{c_{us}}{m_{us}} \\ 0 \end{bmatrix}, \quad B_u = \begin{bmatrix} 0 \\ 0 \\ -\frac{1}{m_{us}} \\ \frac{1}{m_s} \end{bmatrix}$$

$$C_1 = \begin{bmatrix} 0 & -\frac{k_s}{m_s} & \frac{c_s}{m_s} & -\frac{c_s}{m_s} \end{bmatrix}, \quad D_{u1} = \frac{1}{m_s}$$

$$C_2 = \begin{bmatrix} k_{us} & 0 & c_{us} & 0 \\ 0 & 0 & 0 & 0 \end{bmatrix}, \quad D_{u2} = \begin{bmatrix} -c_{us} \\ 0 \end{bmatrix}$$

$$D_{u2} = \begin{bmatrix} 0 \\ 1 \end{bmatrix}$$

## 3 Controller synthesis

In this paper, the  $H_\infty$  controller is proposed. The ride comfort is ensured by constraining the weighted acceleration. On the other hand, the driving stability is improved by suppressing the perturbation of the vertical force.

### 3.1 Frequency weight

The frequency weight used in ISO 2631 has too high dimensions. The frequency weight for the vertical acceleration which has lower dimensions is designed. The frequency weight  $G(s)$  is designed as Eq. (4).

$$G(s) = \frac{1}{3} \cdot \frac{T_1 s + 1}{T_2 s + 1} \cdot \frac{T_4 s + 1}{T_3 s + 1} \quad (4)$$

Here  $T_1$  to  $T_4$  are as follows.

$$T_1 = \frac{1}{3.8}, \quad T_2 = \frac{1}{16}, \quad T_3 = \frac{1}{70.5}, \quad T_4 = \frac{1}{500}$$

The gain diagram of Eq. (4) is shown in Fig. 2. The solid curve is the frequency weight  $G(s)$  used in this study, and the dashed curve is the frequency weight used in ISO 2631-1. It can be seen that the proposed fre-

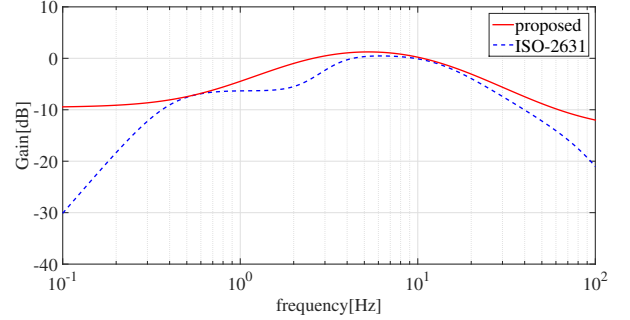


Figure 2 Frequency weight

quency weight  $G(s)$  covers the weight of ISO 2631, and it has the peak at 4-8[Hz].

To adopt this frequency weight to the model, the transfer function  $G(s)$  is translated into the state space representation as Eq. (5).

$$G(s) : \begin{cases} \dot{x}_f(t) = A_f x_f(t) + B_f y_1(t) \\ y_f(t) = C_f x_f(t) + D_f y_1(t) \end{cases} \quad (5)$$

### 3.2 Extended system

The new state variable vector  $\tilde{x}(t)$  for extended system is defined as Eq. (6).

$$\tilde{x}(t) = [ x(t) \quad x_f(t) ]^T \quad (6)$$

Then, the state space representation of the extended system is derived as Eq. (7).

$$\dot{\tilde{x}}(t) = \tilde{A} \tilde{x}(t) + \tilde{B}_w w(t) + \tilde{B}_u u(t) \quad (7)$$

$$\tilde{A} = \begin{bmatrix} A & O^{2 \times 2} \\ B_f C_1 & A_f \end{bmatrix}, \quad \tilde{B}_w = \begin{bmatrix} B_w \\ O^{2 \times 1} \end{bmatrix}$$

$$\tilde{B}_u = \begin{bmatrix} B_u \\ B_f D_{u1} \end{bmatrix}$$

### 3.3 Evaluation output for ride comfort

The evaluation output  $z_1(t)$  which represents the weighted vertical acceleration is defined as Eq. (8)

$$z_1(t) = y_f(t) = \tilde{C}_1 \tilde{x}(t) + \tilde{D}_{u1} u(t) \quad (8)$$

$$\tilde{C}_1 = [ D_f C_1 \quad C_f ], \quad \tilde{D}_{u1} = D_f D_{u1}$$

In ISO 2631-1, the weighted r.m.s. acceleration  $a_w$  is defined as Eq. (9).

$$a_w = \left[ \frac{1}{T} \int_0^T a_w^2(t) dt \right]^{\frac{1}{2}} \quad (9)$$

Here  $a_w(t)$ [m/s<sup>2</sup>] means the weighted acceleration as a function of time. In this paper,  $z_1(t)$  is assumed as  $a_w(t)$ .  $T$ [s] is the duration of the measurement. According to ISO 2631, the ride comfort can be evaluated with the  $a_w$  as Tab. 2.

Table 2 Comfort reactions

Less than 0.315[m/s <sup>2</sup> ]	not uncomfortable
0.315-0.63[m/s <sup>2</sup> ]	a little uncomfortable
0.5-1[m/s <sup>2</sup> ]	fairly uncomfortable
0.8-1.6[m/s <sup>2</sup> ]	uncomfortable
1.25-2.5[m/s <sup>2</sup> ]	very uncomfortable
Greater than 2[m/s <sup>2</sup> ]	extremely uncomfortable

Eq. (10) shows the condition which enable to constraint the weighted r.m.s. acceleration less than the objective value. Here  $a_{wo}$  means the objective value.

$$\begin{aligned} \left[ \frac{1}{T} \int_0^T z_1^2(t) \right]^{\frac{1}{2}} &< a_{wo} \\ \left[ \frac{1}{T} \int_0^T z_1^2(t) \right]^{\frac{1}{2}} &< \frac{a_{wo}}{\left[ \frac{1}{T} \int_0^T w^2(t) \right]^{\frac{1}{2}}} = \mu \\ \|F(s)\|_{\infty} &< \mu \end{aligned} \quad (10)$$

### 3.4 Evaluation output for driving stability

The weight matrix  $W$  is defined as Eq. (11).

$$W = \text{diag}([ w_1 \quad w_2 ]) \quad (11)$$

Here  $w_1$  and  $w_2$  are the weights for the perturbation of the vertical force and the control input, respectively. The evaluation output  $z_2(t)$  is derived as Eq. (12) by using Eqs. (3) and (11).

$$z_2(t) = \tilde{C}_2 \tilde{x}(t) + \tilde{D}_{w2} w(t) + \tilde{D}_{u2} u(t) \quad (12)$$

$$\begin{aligned} \tilde{C}_2 &= [ WC_2 \quad O^{2 \times 2} ], \quad \tilde{D}_{w2} = WD_{w2} \\ \tilde{D}_{u2} &= WD_{u2} \end{aligned}$$

The block diagram of the closed-loop system is shown in Fig. 3.

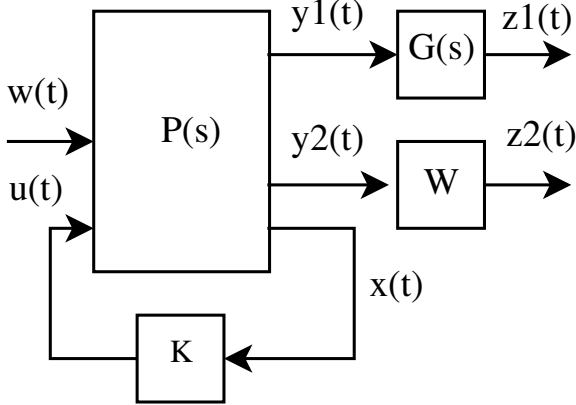


Figure 3 Block diagram

### 3.5 LMI condition

The  $H_{\infty}$  controller is designed to ensure the ride comfort and to improve the driving stability. These problems are formulated to solving following finite set of LMIs. If there exist  $X$  and  $Y$  such that following LMI

conditions are satisfied, the closed-loop system is stabilized by  $u(t) = Kx(t) = YX^{-1}x(t)$  and the upper bound of  $H_{\infty}$  norm is less than  $\gamma$  [4, 6].

minimize :  $\gamma^2$

subject to :

$X > 0$

$$\begin{aligned} \begin{bmatrix} He[\tilde{A}X + \tilde{B}_u Y] & \tilde{B}_w & (\tilde{C}_1 X + \tilde{D}_{u1} Y)^T \\ & \tilde{B}_w^T & -\mu^2 \\ \tilde{C}_1 X + \tilde{D}_{u1} Y & 0 & -1 \end{bmatrix} &< 0 \\ \begin{bmatrix} He[\tilde{A}X + \tilde{B}_u Y] & \tilde{B}_w & (\tilde{C}_2 X + \tilde{D}_{u2} Y)^T \\ & \tilde{B}_w^T & -\gamma^2 \\ \tilde{C}_2 X + \tilde{D}_{u2} Y & \tilde{D}_{w2} & -I^{2 \times 2} \end{bmatrix} &< 0 \end{aligned}$$

## 4 Simulation

In this section, the effectiveness of the proposed controller is evaluated by the simulation.

### 4.1 Simulation setup

In ISO 8608, the road surface profile is defined. For the time-domain analysis, the road surface profile of crass B of is introduced in this study. Fig. 4 shows the road surface profile. The vehicle velocity is assumed as 36.8

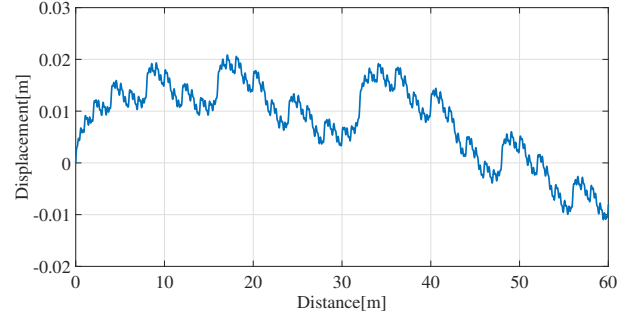


Figure 4 Road surface profile

[km/h].

In this paper, experimental unit which is the scale model of the vehicle is used. The resonance frequency is same, but the amplitude is different. Tab. 3 shows the comparison of the weighted r.m.s. acceleration of the experimental unit value and the real vehicle value [4]. Both of them are the simulation results of the passive suspension. It can be seen that the value of the experi-

Table 3 Experimental unit and real vehicle

Experimental unit	Real vehicle
3.35[m/s <sup>2</sup> ]	0.779[m/s <sup>2</sup> ]

mental unit is 4.3 times larger than the value of the real vehicle. In this paper, "not uncomfortable" of Tab. 2 is the object. the value is modified 4.3 times larger for the experimental unit. Therefore, the objective value  $a_{wo}$  is 1.35. By using these constants, the value of  $\mu$  is 48.3.

On the other hand, the weight matrix  $W$  is chosen as eq. (13).

$$W = \text{diag}([ 0.08 \quad 0.04 ]) \quad (13)$$

The feedback gain  $K$  and the upper bound of  $\gamma$  are obtained as follows.

$$K = [ 3720 \quad -343 \quad 6.20 \quad -264 \quad -94.8 \quad -60.3 ]$$

$$\gamma = 19.4$$

## 4.2 Simulation results

Figs. 5 to 7 show the results of the time-domain analysis. Here the solid curves and the dashed curves mean the results of the active suspension and the passive suspension, respectively.

Fig. 5 show the vertical weighted acceleration of the vehicle body. It can be seen that the maximum amplitude of the weighted acceleration is suppressed by the active suspension. Tab. 4 shows the comparison of the

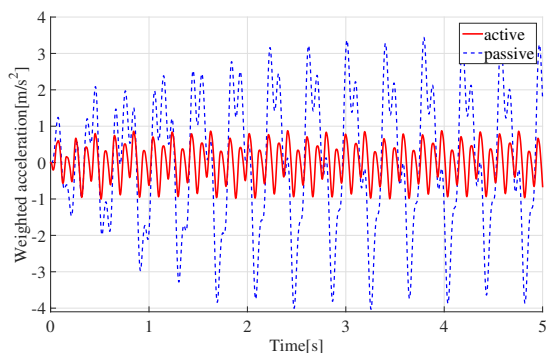


Figure 5 Weighted acceleration1

weighted r.m.s. acceleration of each result. According to Tab. 2, the results are evaluated as not uncomfortable and fairly uncomfortable, respectively. The results indicate that the ride comfort is ensured by the proposed controller.

Table 4 Weighted r.m.s. acceleration

Active	Passive
1.21[m/s <sup>2</sup> ]	3.35[m/s <sup>2</sup> ]

Fig. 6 shows the perturbation of the vertical force of the wheel. The vertical force of the wheel without disturbance is 34[N]. It can be seen that the maximum amplitude of the perturbation of the vertical force is suppressed by the active suspension. The result indicates that the driving stability is improved.

Fig. 7 shows the control input. It can be seen that the control input is less than the limitation of the experimental unit ( $\pm 10$ [v]). The result indicates that the controller can be used in the experiment.

## 5 Conclusion

In this paper, the  $H_\infty$  controller is designed for an active suspension. The main goal of the study is to ensure the ride comfort. The comfort reactions to vibration environment defined in ISO 2631-1 is introduced as the constraint for the weighted r.m.s. acceleration. On the other hand, to improve the driving stability is one of the goal. The perturbation of the vertical force of the wheel is suppressed by considering the deflection of the wheel. The controller is derived by solving the finite set of LMIs. The effectiveness of the proposed controller is

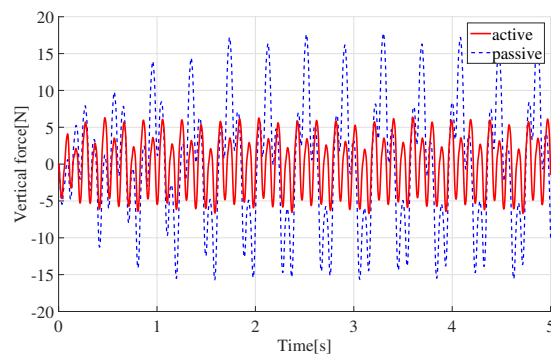


Figure 6 Perturbation of vertical force

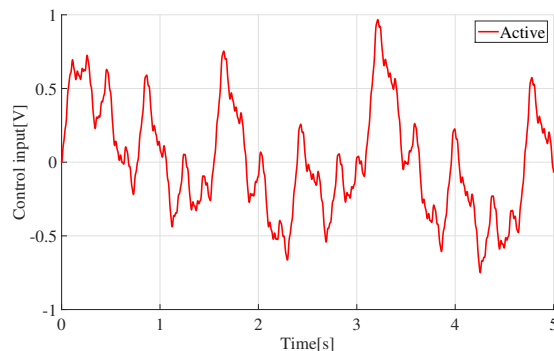


Figure 7 Control input

evaluated by the simulation which uses the road surface profile based on ISO 8608.

## References

- [1] "ISO 2631-1 Mechanical vibration and shock - Evaluation of human exposure to whole-body vibration - Part 1: General requirements", International Organization for Standardization, 1997.
- [2] Y. Hanamura, K. Fujita, Y. Araki, M. Oya, H. Harada, "Control of Vehicle Maneuverability and Stability of 4 Wheeled Vehicle by Active Suspension Control with Additional Vertical Load Control", Transactions of the Japan Society of Mechanical Engineers, Series C 65 (629), pp. 236-243, 1999.
- [3] M. P. Nagarkar, G. J. Vikhe Patil, "Performance Analysis of Quarter Car Active Suspension System: LQR and  $H_\infty$  Control Strategies", 2012 Third International Conference on Computing, Communication and Networking Technologies (ICCCNT'12), 1-6, 2012.
- [4] H. Chen, and K.-H. Guo, "Constrained  $H_\infty$  Control of Active Suspensions: An LMI Approach." IEEE Transactions on Control Systems Technology 13.3, pp. 412-421, 2005.
- [5] "ISO 8608 Mechanical vibration - Road surface profiles - Reporting of measured data", International Organization for Standardization, 2016.
- [6] Y. Kami, E. Nobuya, "Iterative Methods for the Mixed  $H_2/H_\infty$  Control System Design Using  $H_2$  Norm Decreasing Controller Sequences", Transactions of the Society of Instrument and Control Engineers Vol. 40 No. 4, pp. 382-389, 2004.